ON THE MODELLING OF FLEXIBLE ROTOR/MAGNETIC BEARING SYSTEMS WHEN IN CONTACT WITH RETAINER BEARINGS

Mehmet N. Sahinkaya, Abdul-Hadi G. Abulrub, and Patrick S. Keogh
Department of Mechanical Engineering, University of Bath, BA2 7AY, UK
ensmns@bath.ac.uk

ABSTRACT

Magnetic bearings offer many advantages over conventional bearings, but they have to incorporate retainer or backup bearings due to their limited force capacity. Understanding the contact dynamics and controlling the rotor when it is in contact with the retainer bearings are important issues for the successful use of magnetic bearings in safety critical and wider applications. The contact dynamics are complicated and various analysis techniques have been suggested in the literature. These include modelling contact forces as non-linear functions of penetration depth. In this paper, an alternative method based on the constrained Lagrange equations of motion is introduced. Simulation results show its ability to predict a rotor contact orbit with competitive computational efficiency.

INTRODUCTION

Magnetic bearings have to incorporate retainer bearings to protect the rotor and stator laminations. Vibration levels may increase due to power loss, system faults, or sudden changes in system internal and external dynamic properties, such as unbalance [1]. Most controllers are designed by utilising linearised system dynamics, but when the rotor comes into contact with retainer bearings, it enters a highly non-linear state [2]. The system may have to be shut down in order to prevent further damage even if the magnetic bearings are fully functional. Furthermore, extremely high impact forces and high temperatures during the contact cause damage to the retainer bearings.

In some cases, the sudden increase of rotor vibrations, which may cause the contact, is transient or temporary [3]. It may be possible with proper control action to recover rotor position and resume normal contact free operation. This would minimise impact forces and damage to retainer bearings. Also, this would open new application areas, such as land sea and air transportation, where a rotor bearing system may be subjected to sudden external excitation and shutting down the system is not an option. Therefore, efficient modelling of contact dynamics is important for the design of suitable controllers to cope with contact conditions.

The contact dynamics involve several physical factors [4]. The highly non-linear normal contact forces can be estimated using Hertzian theory. The contact forces are represented as functions of displacement of the rotor at the contact point [5], and are related to the rotor penetration depth that increases stiffness of the contact point until the maximum penetration depth is reached [6]. This model suffers from some deficiencies such as physically meaningless negative contact forces [7]. Also, the function is not differentiable at zero penetration. However, a non-linear contact force relationship was implemented that does not exhibit these deficiencies [8]. This paper investigated a case where a rotor drops onto a retainer bearing after sudden failure of the main active magnetic bearing. Another difficulty is the modelling of friction forces. These can be considered to be proportional to the normal forces (Coulomb). However, they may also depend on the relative velocity, surface material properties, displacement, contact geometry and lubrication levels, and behave in a non-linear manner [6, 9]. The Coulomb friction model is used in this paper.

Various experimental and theoretical impact modelling studies have enhanced the understanding of the interaction dynamics of a rotor with a retainer bearing [10]. However, most have suffered from computational inefficiencies. These arise due to the small integration step sizes required to match the high frequency introduced by the high contact stiffness [5, 6, 8]. Instead of trying to model the complicated contact dynamics, an alternative method of based on the constrained Lagrange equations of motion is introduced in this paper. This approach does not require modelling of the contact dynamics. When contact occurs, it is treated as a constraint on the generalised coordinates and the necessary constraint equations are added

through Lagrange multipliers [11]. Constraint forces are then automatically calculated at each integration step and the simulation is switched to a non-contact model as soon as the constraint forces change sign. This would provide an efficient simulation environment to develop and test controllers, which are capable of bringing the rotor back to normal operating conditions. It would eliminate the high numerical stiffness problem associated with conventional modelling of contact forces.

EQUATIONS OF MOTION

The system to be simulated consists of a uniform flexible steel shaft of length 2 m and radius 25 mm, with four 10 kg rigid discs of radii 12 cm. The complete rotor mass of 100 kg is supported by two radial magnetic bearings each with a radial force capacity of 1700 N and a bandwidth of 100 Hz. The magnetic bearing air gaps are 1.2 mm and they are protected with retainer bearings having 0.75 mm radial clearance. A schematic view of the flexible rotor/ magnetic bearing rig is shown in figure 1.

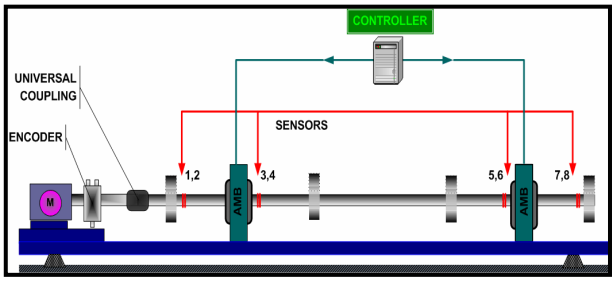

FIGURE 1: Flexible rotor/magnetic bearing rig

The constant speed rotor dynamics are modelled by a 13 lumped mass finite elements with linearised magnetic bearing characteristics:

$$\mathbf{M}\ddot{\mathbf{q}} + \mathbf{C}\dot{\mathbf{q}} + \mathbf{K}\mathbf{q} = \mathbf{F} \tag{1}$$

Here **M**, **C** and **K** are the mass, damping and stiffness matrices of the rotor/magnetic bearing system, which includes local proportional and derivative (PD) feedback. The input vector **F** represents external disturbances including unbalance forces. The generalised displacement vector **q** contains linear and angular deflections at nodal positions. This gives four degrees of freedom for each node and **q** can be written

$$\mathbf{q}^T = [\mathbf{x}^T, \mathbf{y}^T, \boldsymbol{\theta}^T, \boldsymbol{\varphi}^T] \tag{2}$$

where **x** and **y** denote the linear displacement vectors in orthogonal X-Y axes, and **θ**, **φ** denote angular displacement vectors about the X-Y axes respectively.

If the rotor comes into contact with retainer bearings, the force vector **F** in equation (1) must be modified to include the contact forces. These will be applied to nodes corresponding with the retainer bearing locations. The external force vector can be written as

$$\mathbf{F} = \mathbf{F_{ob}} + \mathbf{B_C}\mathbf{F_C} \tag{3}$$

where $\mathbf{F_{ob}}$ is the out-of balance force vector, $\mathbf{B_C}$ is a contact force coefficient matrix specifying the contact locations, and $\mathbf{F_C}$ represents the contact forces.

MODELLING OF CONTACT FORCES

The classical method of calculating contact forces is to utilise the Hertzian theory [12]. When contact occurs, the normal contact force induced is a function of the contact stiffness K_c and contact damping C_c, and related to the rotor penetration depth δ. A simple method is to use linear contact force expression [5]:

$$F_n = \begin{cases} K_C\delta & ,\delta > 0 \\ 0 & ,\delta \le 0 \end{cases} \tag{4}$$

Alternative formulations use non-linear expressions [8]. However, whatever expression is used, the contact force calculation as a function of δ introduces very high stiffness. This introduces high frequency behaviour and hence requires longer computation time. Therefore, equation (4) is used to compare the computational efficiency with the approach developed in this paper. The benefits in terms of the computational efficiency will be demonstrated on the simulated flexible rotor magnetic bearing system described in the previous section.

CONSTRAINT LAGRANGIAN FORMULATION

When contact occurs, say, at node k, it can be treated as a constraint on the generalised co-ordinates through

$$f_1 = c^2 - x_k^2 - y_k^2 = 0 \tag{5}$$

where c is the retainer bearing clearance. This holonomic constraint reduces the number of degrees of freedom by unity. If contact occurs at another node simultaneously, a second constraint equation similar to equation (5) must be introduced. In general, the constrained matrix dynamic equation of the system can be written as

$$\mathbf{M}\ddot{\mathbf{q}} + \mathbf{C}\dot{\mathbf{q}} + \mathbf{K}\mathbf{q} + \mathbf{J}^T\boldsymbol{\lambda} = \mathbf{F} \tag{6}$$

The constraint Jacobian matrix **J** contains the partial derivatives of the constraint equations with respect to generalised coordinates. The Lagrange multiplier vector **λ** has a dimension equal to the number of constraint equations. Introduction of **λ** increases the number of variables and additional equations are needed. These equations can be obtained by differentiating the constraint equations twice with respect to time giving the following equations of motion for the contact case [11]:

$$\begin{bmatrix} \mathbf{M} & \mathbf{J}^T \\ \mathbf{J} & \mathbf{0} \end{bmatrix} \begin{bmatrix} \ddot{\mathbf{q}} \\ \boldsymbol{\lambda} \end{bmatrix} = \begin{bmatrix} \mathbf{F_{ob}} - \mathbf{C}\dot{\mathbf{q}} - \mathbf{K}\mathbf{q} \\ \mathbf{D}(\mathbf{q}, \dot{\mathbf{q}}) \end{bmatrix} \tag{7}$$

This gives the correct number of equations to solve for the acceleration vector and the Lagrange multipliers. The vector **D** contains the velocity and displacement related terms arising from the double differentiation. By defining a state vector **z** as follows:

$$\mathbf{z}^T = [\mathbf{q}^T, \dot{\mathbf{q}}^T] \tag{8}$$

the second order algebraic-differential equations (7) can be converted to a system of first order differential equations as follows:

$$\dot{\mathbf{z}} = \begin{bmatrix} \mathbf{z_2} \\ \ddot{\mathbf{q}}(\mathbf{z_1}, \mathbf{z_2}) \end{bmatrix} \tag{9}$$

where $\ddot{\mathbf{q}}(\mathbf{z_1}, \mathbf{z_2})$ is solved from equation (7). Equation (9) can be solved with any suitable integration algorithm. This approach does not require the modelling of the contact forces, which are automatically eliminated from the equations. However, the contact forces are equal to the constraint forces, which hold the rotor to the constraint. The constraint forces are defined as

$$\mathbf{F_C} = -\mathbf{J}^T \boldsymbol{\lambda} \tag{10}$$

When contact occurs, the constraint (or contact) forces will be directed to the centre of the rotor and hence will keep the rotor at the clearance limit. If the contact forces change direction, the simulation should be switched to the non-constrained case as given by equation (1). Therefore the whole process involving contact and non-contact models can be automated with two switches. The non-contact model should be executed for as long as the constraint equations are positive (i.e. $f_1 > 0$) and will switch to the contact model at the crossing point of $f_1 = 0$ and negative slope. The contact model will then run for as long as the contact force is towards the centre of the clearance circle, and will switch back to the non-contact model if the contact force changes direction at zero crossing. A friction force can easily be added as a function of the normal component of the contact force. The one important issue when changing from one model to another is the calculation of the initial conditions, which will be discussed in the following example.

Figure 2 shows the coordinate system at a contact node, say node k. The shaft centre whirls around the bearing centre as described by the variables x_k and y_k. The shaft also rotates with a constant speed Ω.

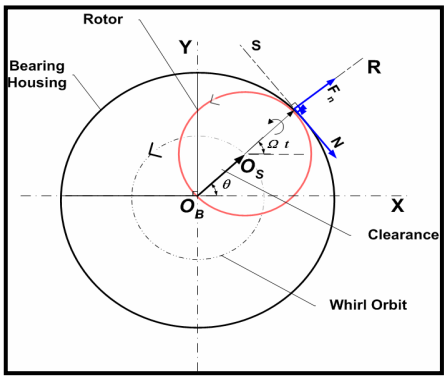

FIGURE 2: System axes at the contact node

Since contact involves normal and tangential force components, it is convenient to work with the rotating R-S axes rather than the fixed X-Y axes. The coordinate transformation at any given point in time can be accomplished by using the following direction cosine matrix:

$$\alpha = \begin{pmatrix} \cos\theta & -\sin\theta \\ \sin\theta & \cos\theta \end{pmatrix} \tag{11}$$

where

$$\theta = \tan^{-1}(y_k / x_k) \tag{12}$$

The first and second derivatives of the constraint equation (5) are:

$$\begin{aligned} \dot{f}_1 &= -2x_k\dot{x}_k - 2y_k\dot{y}_k = 0 \qquad (a) \\ \ddot{f}_1 &= -2x_k\ddot{x}_k - 2y_k\ddot{y}_k - 2\dot{x}_k^2 - 2\dot{y}_k^2 = 0 \qquad (b) \end{aligned} \tag{13}$$

The Jacobian **J** is a row vector and the right hand side matrix **D** is now a scalar for this case:

$$\begin{aligned} \mathbf{J} &= [0 \ldots -2x_k \, 0 \ldots -2y_k \ldots 0] \\ \mathbf{D} &= 2\dot{x}_k^2 + 2\dot{y}_k^2 \end{aligned} \tag{14}$$

The constraint (or contact) forces can then be calculated from equation (10):

$$F_{C,x} = 2x_k\lambda_1$$
$$F_{C,y} = 2y_k\lambda_1 \qquad (15)$$

Converting these forces into the R-S frame and taking the R component gives the normal contact force. This is negative when contact occurs. A zero crossing before this force changes sign signals the end of the contact. The state values at the crossover can be used as initial conditions for the non-contact model.

Consider now the switch from a non-contact to contact model. The setting of the initial conditions for the contact model is more involved. When zero crossover occurs, the state variable values satisfy only the constraint equation, but not the first derivative of the constraint equation (13a). The second derivative of the constraint is automatically satisfied through the solution of equation (7). To set the initial velocities for x_k and y_k, it is again beneficial to consider the components of the impact velocity in the R-S directions. The radial component of the velocity must be set to zero as implied by equation (13a). It is logical to keep the same tangential component, although this could be set to another value appropriate to physical conditions.

Frictional forces are proportional to the normal contact forces. However, they are also correlated to the relative velocity between the rotor and the bearing. This relative velocity v between the surfaces can be calculated as

$$v = R_s\Omega + (R_b - R_s)\dot{\theta} - R_b\Omega_b \qquad (16)$$

where R_s and R_b denote the radius of the shaft and the bearing respectively, and Ω_b is the rotational speed of the inner surface of the bearing (for rolling element bearings). A friction force F_f can then be represented as

$$F_f = \text{sgn}(\nu)\times\mu\times F_n \quad for\ \nu \neq 0 \qquad (17)$$

where F_n is normal component of the contact force and μ denotes the dynamic coefficient of friction. In the following results, it is assumed that the bearing housing does not rotate (i.e. $\Omega_b = 0$), and no stiction exists.

SIMULATION RESULTS AND DISCUSSION

A sudden increase in out of balance is used to initiate contact with the non-driven end retainer bearing (figure 1) at different rotational speeds. The out of balance is added to the disk at the non-driven end of the rotor. Initially, the simulation is run with a small out of balance force until a steady state motion is achieved before the out of balance is increased further. After a pre-defined period, the out of balance is reduced to the initial value to show that the rotor returns to its original non-contacting steady state orbit. A typical run is simulated at a rotational speed of Ω = 90 rad/s and the resulting orbit is shown in figure 3. A critical speed involving significant first order rotor flexure is about 150 rad/s. The initial unbalance of 0.02 kgm was suddenly increased to 0.1 kgm to cause the contact. The radial position of the rotor and the contact forces as calculated by the constrained Lagrangian model are shown in figure 4. This produces contact forces as high as 1.8 kN, settling down with peaks of around 700 N before the rotor returns to a non-contacting state.

Figures 5 and 6 show the results for a higher steady rotational speed of 190 rad/s, which is above the first flexural mode critical speed. The initial unbalance was 0.01 kgm before being increased to 0.03 kgm. Bouncing motion is clearly observed with contact forces up to 2.2 kN.

The results and the orbit shapes obtained by the constrained Lagrangian formulation are in agreement with those experienced by other researchers [7, 13]. However, the main benefit of using this approach is the computational efficiency. To demonstrate this point, the same simulations were run using the classical contact model given in equation (4). The contact forces, which depend on the selection of contact stiffness properties, were smaller than the forces predicted by the constrained Lagrangian formulation. A typical run at 190 rad/s with a relatively high stiffness value of K_c = 1.25×10^{12} N/m takes approximately 716 seconds computation time for one rotational cycle after the first incidence of contact. By comparison, the constrained Lagrangian method takes about 13.3 seconds per cycle of simulation. The maximum contact force of 0.9 kN predicted by the conventional model is lower than the 1.8 kN predicted by the constrained Lagrangian formulation. The computational time can be improved by selecting a lower K_c value for the contact stiffness. For example, using K_c = 1.25×10^{10} N/m reduces the computational time to about 331 seconds per cycle of simulation in contact with the predicted maximum contact force of 85 N. The constrained Lagrangian predicts the upper limit of contact force possible for any type of retainer bearing. This is due to the fact that the constraint considers the nominal radial clearance as an absolutely rigid boundary for rotor excursions. The orbit and the contact forces predicted by the high stiffness case when K_c = 1.25×10^{12} N/m at 90 rad/s are shown in figures 7 and 8 respectively. They are of a similar nature to those shown in figures 3 and 4.

CONCLUSIONS

A variety of techniques for modelling contact dynamics have been suggested in the literature, including modelling contact forces as non-linear functions of penetration at the contact point. Most of these techniques introduce numerical inefficiencies during the integration of the high order flexible rotor equations of motion and high numerical stiffness associated with the contact equation. The method presented in this paper, based on the constrained Lagrangian formulation, overcomes these difficulties.

The constrained Lagrangian equations of motion do not require the modelling of the contact forces. These are eliminated by the constraints. When contact occurs, a constraint on the generalised coordinates and the constrained equations is added to the equations of motion through Lagrange multipliers. Contact forces may then be calculated using the Lagrange multipliers, which are evaluated during the solution of algebraic-differential equations of the system. The direction of the constraint forces determines the transition from a contact state to a non-contact state. The treatment of initial conditions is needed when initiating the contact model. Numerical stiffness associated with classical representation of contact forces is avoided. Simulation examples were used to assess the level of computational efficiency of the proposed technique.

It is anticipated that the technique will be of use in future real time estimation of contact forces for application in the design of position control algorithms.

ACKNOWLEDGEMENT

The authors acknowledge the support of the Engineering and Physical Sciences Research Council of the U.K. through Grant GR/R45277/01.

REFERENCES

1. **G. Schwetizer, H. Bleuler and A. Traxler,** "*Active Magnetic Bearings Basics, Properties and Application of Active Magnetic Bearings*", 1994, Zurich, vdf Hochschulverlag AG.
2. **A. Muszynska,** "*Rotor-to-Stationary Part Full Annular Contact Modelling*", Proceedings 9th Int. Symposium on Transport Phenomena and Dynamic of Rotating Machinery, Hawaii, 10-14 February 2002.
3. **P. S. Keogh, C. Mu and C. R. Burrows,** "*Optimized Design of Vibration Controllers for Steady and Transient Excitation of Flexible Rotors*", 1995, Proc. Instn. Mech. Engrs, Part **C,** Journal of Mechanical Engineering Science, Vol. 218, pp 155-168.
4. **S. Faik and H. Witteman,** "*Modelling of Impact Dynamics: A Literature Survey*", Proceedings International ADAMS User Conference, 2000.
5. **H. Xie, G. T. Flowers, L. Feng and C. Lawrence,** "*Steady-State Dynamic Behaviour of a Flexible Rotor with Auxiliary Support from a Clearance Bearing*", 1999, ASME Journal of Vibration and Acoustics, Vol. 121, pp 79-83.
6. **R. G. Kirk, K. V. S. Raju and K. Ramesh,** "*Modelling of AMB Turbo-machinery for Transient Analysis*", 1997, Proceeding of MAG's, Alexandria, USA, pp 139-153.
7. **G. von Groll and D. J. Ewins,** "*A Mechanism of Low Sub-harmonic Response in Rotor/Stator Contact Measurements and Simulations*", 2002, ASME Journal of Vibration and Acoustics, Vol. 124, pp 350-358.
8. **M. Fumagalli and G. Schweitzer,** "*Measurements on a Rotor Contacting Its Housing*", Proceedings of Instn. Mech. Engrs 6th International Conference on Vibrations in Rotating Machinery, 9-12 September 1996, Oxford. Paper No. C500/085/96.
9. **H. Olsson, K. Åström, C. Wit, M. Gäfvert and P. Lischinsky,** "*Friction Models and Friction Compensation*", 1998, European Journal of Control, Vol. 3, pp 176-195.
10. **T. Ishii and R. G. Kirk,** "*Transient Response Technique Applied to Active Magnetic Bearing Machinery During Rotor Drop*", 1996, ASME Journal of Vibration and Acoustics, Vol. 118, pp 154-163.
11. **M. N. Sahinkaya, "***Inverse Dynamic Analysis of Multi-Physics Systems*", 2004, Proc. Instn. Mech. Engrs, Part **I,** Journal of Systems and Control Engineering, Vol. 218, pp 13-26.
12. **K. L. Johnson,** "*Contact Mechanics*", 1985, Cambridge University Press.
13. **F. Wu and G. T. Flowers,** "*An Experimental Study of the Influence of Disk Flexibility and Rubbing on Rotor Dynamics*", Proceedings, DE-Vol. 60, ASME Conference on Vibration of Rotating Systems, September 1993.

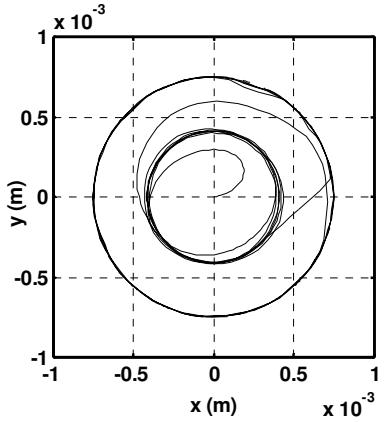

FIGURE 3: Rotor orbit response at 90 rad/s

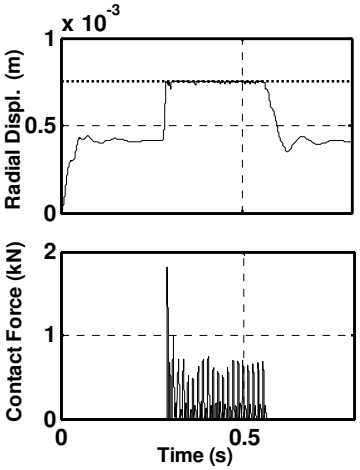

FIGURE 4: Radial displacement and contact force at 90 rad/s

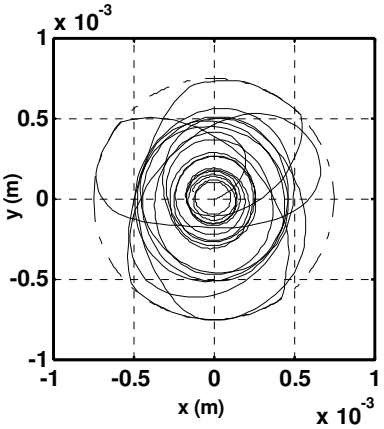

FIGURE 5: Rotor orbit response at 190 rad/s

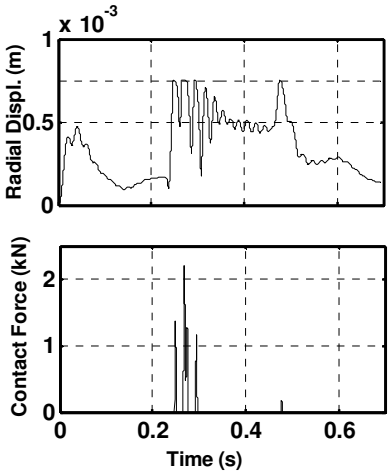

FIGURE 6: Radial displacement and contact force at 190 rad/s

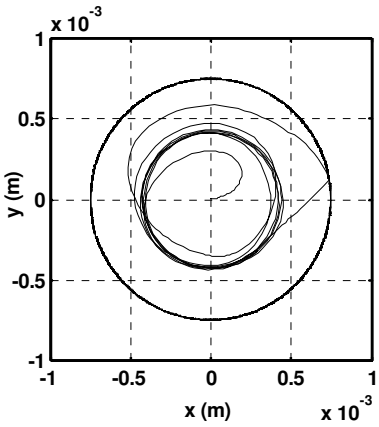

FIGURE 7: Rotor orbit response at 90 rad/s with classical contact model K_c=1.25×10^{12} N/m

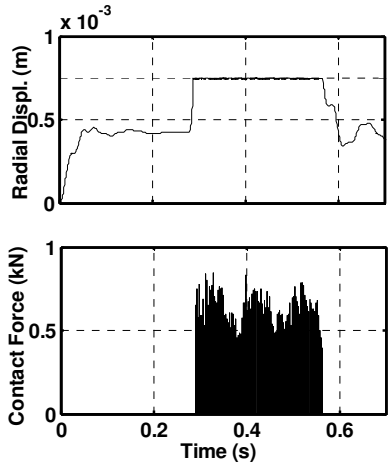

FIGURE 8: Radial displacement and contact forces at 90 rad/s with classical contact model K_c = 1.25×10^{12} N/m